

Dynamics of the Super ACO FEL measured with a double sweep streak camera

R.Roux^{1,2}, R. J. Bakker^{1,2}, M. E. Couprie^{1,2}, A. Delboulbé², D. Garzella², L. Nahon^{1,2}, D. Nutarelli^{1,2}, B. Visentin^{2,4}, M. Billardon^{2,3}

1 CEA/SPAM, centre d'étude de Saclay, 91191 Gif-sur-Yvette, France

2 LURE, bat. 209D, Université Paris Sud, 91405 Orsay cedex, France

3 ESPCI, 10 rue Vauquelin, 75231 Paris cedex, France

4 CEA/LNS, centre d'étude de Saclay, 91191 Gif-sur-Yvette, France

ABSTRACT

The temporal evolution of the Super-ACO storage ring Free Electron Laser (FEL) is followed with a double sweep streak camera : sub-micropulses can be observed, together with drifts of the laser position with respect to the electron beam.

INTRODUCTION

Temporal measurements with detectors more and more accurate have been driven on the FEL in order to better understand the FEL dynamics and to improve its stability. Such an issue is especially critical during users experiences with the FEL [1].

1 USUAL BEHAVIOUR OF THE FEL

The Super-ACO FEL is generally operated at the nominal energy of the ring, i.e., 800 MeV, between 30-120 mA in two bunches around 350 nm. The laser effect is produced when the round-trip of the light pulses in the optical resonator is synchronized with the positron bunch circulation in the ring. The first order of this interaction leads to a micro-bunching of the bunch and the average energy given to the laser wave is zero. At the second order, because the laser wavelength is a little bit above the resonance wavelength, by damping of electrons energy (because of laser electric field), microbunches emit coherent radiation. But, due to the laser electric field growth, the electron energy spread increases, inducing a lengthening of the bunch and then a laser gain reduction. So, this competition between the laser intensity and the energy spread growth drives to the laser power saturation. The laser temporal structure adopts different regimes depending of the detuning (longitudinal desynchronization) between laser pulse and electrons bunch as shown in figure 1 [3].

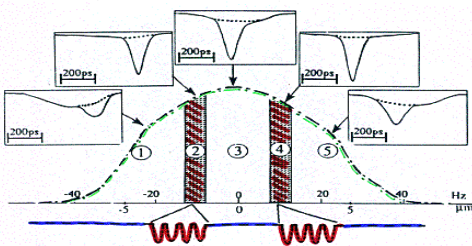


Figure 1 : The detuning curve represents laser intensity (dashed line) versus desynchronization between laser pulse and electrons bunch, i.e. a cavity length change of 0.18 mm is equivalent to modification of the revolution frequency of 1 kHz. Curves in frames above the detuning curve (full lines : FEL and dotted lines : stored synchrotron radiation) represent microtemporal structure and the lower curve the macrotemporal structure of the FEL in each area.

One can distinguish five areas with respect to the temporal structure. At perfect synchronism, the laser is continuous at the ms scale and has the shortest temporal width (between 20-60 ps FWHM) and the highest intensity but presents a jitter up to 150 ps. From each side (areas 2 and 4), the laser is pulsed with less intensity and its temporal width is wider. Then, with a larger detuning (areas 1 and 5) the laser becomes again cw, less intense and its width is increased.

It then appears that operating the FEL at perfect synchronism corresponds to the optimum situation for users experiments. However, the natural micropulse jitter in its longitudinal position can drive the laser outside the central area toward pulsed areas inducing sudden variations of the intensity and enhancing laser temporal width. These characteristics have been observed with various detectors described in the next section.

2 DIAGNOSTICS

So far, the laser pulse temporal distribution in the ps range was analysed with a stroboscopic detector (of resolution 10 ps) so called the dissector [3] and with a Thomson single sweep streak camera [4]. The dissector allowed to monitor the average distribution of the FEL and the electrons bunch distribution and also showed the jitter of the FEL micropulse, partially responsible of the saturation process of the laser [5]. Besides, a longitudinal feedback system [6] compensates this jitter down to 20 ps by monitoring the FEL micropulse position at 300 Hz with the dissector and reacting on the synchronism condition. Single sweep streak camera of resolution 5 ps [4] allowed to measure whole distribution of one single laser pulse : it could exhibit several micropulses in the same micropulse. However it was not possible to follow its evolution in time.

For that purpose a Hamamatsu Double Sweep Streak Camera C5680 (DSSC) with a 2 ps resolution has been

recently installed. In addition to the vertical fast sweep, a horizontal slow sweep shift light pulses on the CCD screen versus 12 sweep time available between one μ s and one s. Hence one can measure the evolution of the temporal distribution of one laser micropulse. This is fundamentally different from the results obtained with the dissector which only permits to measure the light pulses temporal distribution averaged over 3.3 ms.

3 TEMPORAL EVOLUTION OF THE FEL

With the DSSC, the laser shape (width, substructure) and the jitter have been measured in the different areas of the detuning curve below 60 mA, the threshold for coherent quadrupolar synchrotron oscillation. Each image is composed of 480 horizontal lines over 640 vertical lines, i.e., for a horizontal time axis of 10 ms one vertical line already represents 15.625μ s in the horizontal time equal to 130 light pulses.

Intensity profiles are provided by horizontal or vertical slices in the image, i.e., during a specific space of time the micropulse temporal distribution of the vertical lines have been averaged. The same method is applied to obtain laser intensity versus horizontal time axis.

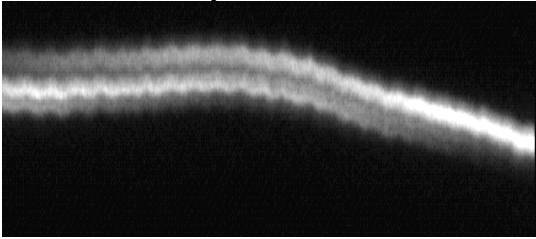


Figure 2 : cw laser in the area 3. Horizontal time axis : 10 ms (one vertical line represents 15.625μ s in the horizontal time, i.e. 130 light pulses), vertical time axis : 700 ps, $I = 50$ mA. The zero for the horizontal axis is on the left side.

Figure 2, recorded for the laser in zone 3, shows two continuous lines which drift together : at this scale the laser being cw, they represent two sub-micropulses of equal intensity vs time (slow time sweep of 10 ms). At the beginning, the upper sub-micropulse is much less intense than the other. After 4 ms, they have equal intensity whereas after 8 ms, the lower one gets dominant. An example of a vertical intensity profile is showed in figure 3. The evolution at the ms scale of the laser temporal width is presented in figure 4.

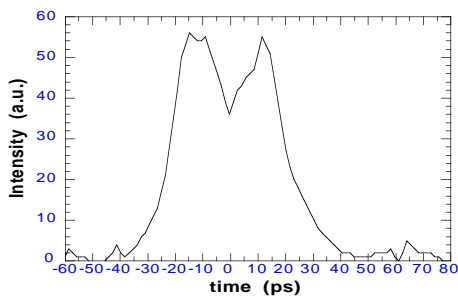


Figure 3 : temporal distribution of the laser micropulse showing two sub-micropulses averaged over 15.625μ s (equal to 130 light pulses) at 5 ms on the horizontal axis.

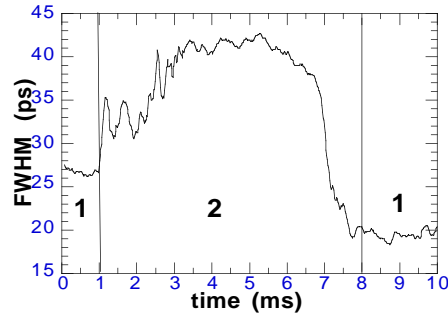


Figure 4 : evolution of the laser micropulse width and the number of sub-micropulses in each zone. The calculated FWHM for each vertical line is integrated over 15.625μ s. It reproduces the evolution of sub-micropulses. Small values correspond to 1 micropulse (as between 0-1 ms and 7.5-10 ms) and higher values to 2 sub-micropulses (between 3-6 ms).

Finally the mean width (FWHM) of the sub-micropulse (averaged between 7.5-10 ms) and the total micropulse (averaged between 3-6 ms) are $19.5 \text{ ps} \pm 0.5 \text{ ps}$ and $41.3 \text{ ps} \pm 0.7 \text{ ps}$, respectively. We could estimate a sub-micropulse lasts over a period of approximately 20 ns. The total micropulse width is narrowed by a factor 10 compared to the electron bunch (444 ps measured at that current) and the sub-micropulse width by a factor 20.

If the laser pulse and the electron bunch are slightly desynchronised, the laser becomes pulsed at the millisecond scale with a period related to the laser rise time and the synchrotron damping time (see figure 5).

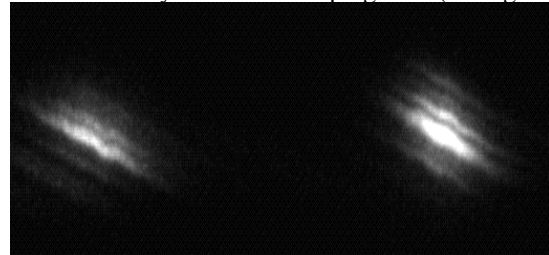


Figure 5 : pulsed laser in area 4. Horizontal time scale : 10 ms, vertical time scale : 700 ps, $I = 35.4$ mA.

Figure 5, one see 2 macropulses which inside show five sub-micropulses which drift together.

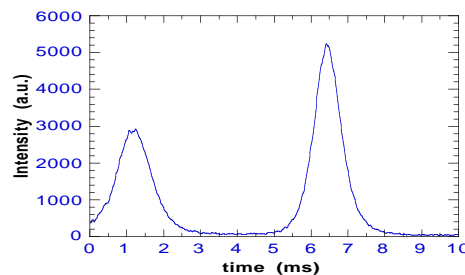


Figure 6 : Curve of the laser intensity versus horizontal time showing 2 macropulses of 1.11 ms and 0.86 ms FWHM separated by 5.28 ms.

As for the laser in the area 3, we have plotted the width of the laser micropulse temporal distribution versus horizontal time (figure 7).

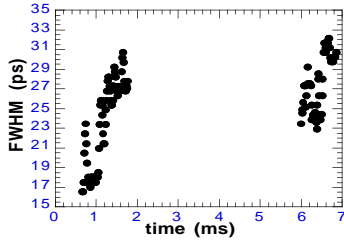


Figure 7 : laser micropulse FWHM versus horizontal time averaged over $15 \mu\text{s}$.

As in former case, the width of one sub-micropulse is enhanced by the growing of others.

If the laser pulse and the electron bunch are further desynchronised, the laser becomes again cw (see figure 8) because the laser operates at the threshold of the lasing [2].

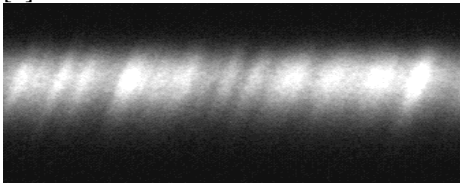


Figure 8 : cw laser in the area 5, horizontal time scale : 10 ms, vertical time scale : 700 ps, $I = 57 \text{ mA}$.

The laser behaviour is much more stable on the macrotemporal scale but the width of the laser micropulse distribution is enhanced by a factor 10, over the sub-micropulse width in area 3, without any sub-micropulses. The laser micropulse width only oscillates very quickly around its mean value, due to statistics of measurements when sub-micropulses are absent. The mean FWHM is about $103.5 \pm 4.7 \text{ ps}$, five times the width of one sub-micropulse in the area 2 or 3. All values, for each laser regime, are summarised in table 1.

zone	$\tau_{\text{sub}}(\text{ps})$	$\tau_{\text{tot}}(\text{ps})$	$\Delta(\text{ps/ms})$
3	19.5 ± 0.5	41.3 ± 0.7	16.5
4	18 ± 0.5	28 ± 2	22.2
5		103.5 ± 4.7	0

Table 1 : τ_{sub} and τ_{tot} represent the FWHM of laser sub-micropulses and total micropulse, respectively. Δ stands for the drift speed.

The sub-micropulses have the same width approximately but not the same total micropulse width in zone 3 and 4. It is due to the fact that, in the pulsed regime, sub-micropulses intensity is not equal as in the cw regime. The cw laser seems to be more stable than the pulsed laser because the drift speed is lower. Besides, due to its larger width, the laser in zone 5 is not attractive although its good stability. With a spectral bandwidth of 0.3 \AA for 350 nm of wavelength and about 20 ps of temporal width in zone 3, the laser is very near the Fourier limit (12 ps of temporal width for 0.3 \AA of spectral width). Besides, one observed drifts of the sub-micropulses (see fig. 2) and surprisingly, with a constant total intensity balanced in the 2 sub-micropulses. Moreover, the jitter can be enough high to push the laser in a pulsed area (figure 10).



figure 10 : cw laser becoming pulsed, horizontal time scale : 10 ms, vertical time scale : 700 ps, $I = 35 \text{ mA}$.

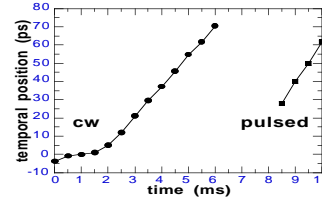


Figure 11 : microtemporal position of a laser sub-micropulse versus horizontal time (averaged over $15 \mu\text{s}$).

The cw laser does not move at the beginning (area 3), then it moves linearly with time since 1.5 ms until 6 ms. Between 6 and 8.5 ms, there is no laser and it starts again since 8.5 ms until 10 ms. The drift speed, defined as the ratio between the displacement of the laser temporal position and the macroscopic time used, is given by curve slopes of the figure 11. So, the drift speed of the cw laser is 16.5 ps/ms and 22.2 ps/ms for the pulsed laser. Therefore the cw laser moved itself 74 ps which is enough to bring it in the pulsed area. In fact this jitter represents another way for the laser saturation. Classically, the saturation results from the competition between the growth of the laser intracavity power and the increase of the beam energy spread inducing a lengthening of the electron bunch, i.e., a reduction of the laser gain. In addition, the laser drift implies a reduction in the electronic density interacting with the laser pulse and therefore it leads to a laser gain reduction.

4 CONCLUSION

Various measurements are under way in others modes of the FEL but not reported here. The DSSC is a very useful tool for the characterisation of the FEL dynamics which understanding is required for the quality of FEL sources. Besides, more precise theory will benefit such knowledge and apply for future projects design.

5 REFERENCES

- [1] M. E. Couprie, F. Merola, P. Tauc, D. Garzella, A. Delboulb , T. Hara, and M. Billardon, Rev. Sci. Instrum. **65** (5), May 1994.
- [2] M. E. Couprie, M. Velghe, R. Prazeres, D. Jaroszynski, and M. Billardon, Phys. Rev. A **44**, 1301 (1991).
- [3] D. A. G. Deacon, L. R. Elias, J. M. J. Madey, G. L. Ramian, H. Schwettman, and T. I. Smith, Phys. Rev. Lett. **38**, 892 (1977).
- [4] M. E. Couprie, T. Hara, D. Gontier, P. Troussel, D. Garzella, A. Delboulb , and M. Billardon, Phys. Rev. E **53**, 2 (1996).
- [5] M. Billardon, D. Garzella, and M. E. Couprie, Phys. Rev. Lett **69**(16), 2368 (1992).
- [6] M. E. Couprie, D. Garzella, J. H. Codarbox, and M. Billardon, Nucl. Instrum. Methods A **358**, 374 (1995).